Optimal Scheduling of Microgrid-Based Virtual Power Plants Considering Demand Response and Capacity Withholding Opportunities

Mostafa Tabatabaei, Mehrdad Setayesh Nazar
Fac. of Elect. Eng., Shahid Beheshti Univ. Tehran, Iran
se_tabatabaei@sbu.ac.ir; m_setayesh@sbu.ac.ir

Miadreza Shafie-khah
School of Tech. and Innov. Univ. of Vaasa
Vaasa, Finland
miadreza@gmail.com

Gerardo J. Osório
Portucalense Univ. Infante D. Henrique, Porto, Portugal
and C-MAST, Univ. Beira Interior, Covilha, Portugal
gerardo@upt.pt

João P. S. Catalão
FEUP and INESC TEC
Porto, Portugal
catalao@fe.up.pt

2021 IEEE Madrid PowerTech | 978-1-6654-3597-0/21/$31.00 ©2021 IEEE | DOI: 10.1109/PowerTech46648.2021.9494964

***Abstract*—This work addresses a stochastic framework for optimal coordination of a microgrid-based virtual power plant (VPP) that participates in day-ahead energy and ancillary service markets. The microgrids are equipped with different types of distributed energy resources. A two-stage optimization formulation is proposed to maximize the benefit of the virtual power plant and minimize the energy procurement costs of the Distribution System Operator (DSO). The proposed model determines the optimal commitment scheduling of energy resources, considering the capacity withholding opportunities of the VPP that should be detected by the DSO. To evaluate the effectiveness of the proposed model, the algorithm is assessed for the 123-bus IEEE test system. The results show that the proposed method successfully maximizes the virtual power plant profit considering capacity withholding penalties.**

***Keywords*—Demand response, Distributed energy resources, Microgrid, Stochastic optimization, Virtual power plant.**

I. INTRODUCTION

Virtual power plant (VPP) is a conceptual framework for the coordinated operation of multiple energy resources. The VPP can consist of multiple microgrids (MGs) and/or multiple fuel-based energy conversion facilities. The VPP can coordinate the bidding strategies of MGs in energy and ancillary service markets [1].

Many studies have been performed on the optimal scheduling of VPPs and some of them have considered the multi-MGs bidding strategy problem. Ref. [1] has presented an optimal scheduling algorithm for a VPP that participated in energy and ancillary services. The contingencies and demand response processes were considered in the proposed conditional value-at-risk (CVaR) model.

Ref. [2] introduced a bi-level algorithm for finding the optimal bidding of VPP in the day-ahead market and minimizing the penalty costs of mismatches in the real-time market. The master and client problems were solved using modified genetic algorithm and mixed integer optimization processes, respectively. Ref. [3] has introduced a linear optimization framework for optimal scheduling of VPP that consisted of a two-level stochastic optimization process. The algorithm determined the optimal dispatch of VPP energy resources in the first level problem and the balancing market decision variables were optimized in the second level problem.

Ref. [4] has proposed a three-stage optimization algorithm for multi-energy carrier VPP that participated in different electricity markets. The first stage problem minimized the energy costs of the system; meanwhile, the second stage problem solved the economic dispatch problem for the intra-hour market. The third stage problem determined the optimal system dispatch for the real-time market. Ref. [5] has assessed an optimization model for multi-objective optimization of the VPP scheduling problem that considered electric vehicles, variable/stochastic electricity generation facilities, and fossil-fueled electricity generation facilities. The objective function comprised revenue of VPP and penalty costs that were solved by a chance-constrained optimization procedure.

Ref. [6] has proposed a two-stage algorithm for optimizing the scheduling of VPP for different operational horizons. The first stage problem optimized the intra-day electricity exchange of VPP with the market and the second stage problem minimized the operational variable mismatches. Ref. [7] has introduced a model for revenue optimization of VPP in the day-ahead market considering load, price, and energy generation uncertainties. The particle swarm optimization was utilized to solve the stochastic model.

Ref. [8] has proposed a bi-level optimization algorithm for scheduling of VPP considering different sources of uncertainties. The first-stage problem optimized the bidding strategy of VPP; meanwhile, the second-stage problem determined the economic dispatch of system decision variables. Ref. [9] has introduced a CVaR model for maximizing the revenue of VPP in day-ahead energy and ancillary service markets. The uncertainties of electric vehicles, intermittent electricity generation facilities, and market prices were modeled.

Ref. [10] has evaluated a two-stage nonlinear optimization algorithm for dispatching of VPP energy resources. The master problem maximized the VPP revenues and the client problem minimized the energy purchasing costs of the system. Ref. [11] has assessed a two-stage VPP scheduling algorithm that modeled the uncertainties of electricity generation facilities. The first stage problem maximized the revenue of VPP and the second stage problem minimized the energy purchasing costs of the system.

G.J. Osório acknowledges the support from Portuguese national funds by FCT - Foundation for Science and Technology, within C-MAST - UIDB/00151/2020. Also, J.P.S. Catalão acknowledges the support by FEDER funds through COMPETE 2020 and by Portuguese funds through FCT, under POCI-01-0145-FEDER-029803 (02/SAICT/2017).

978-1-6654-3597-0/21/$31.00 ©2021 IEEE

Authorized licensed use limited to: b-on: UNIVERSIDADE DO PORTO. Downloaded on July 30,2021 at 17:19:45 UTC from IEEE Xplore. Restrictions apply.

A robust optimization model was utilized for solving the problem.

In [2-11], the impacts of capacity withholding index on the microgrid-based VPP optimal day-ahead scheduling problem were not considered. The present work utilizes a stochastic mixed-integer programming method to consider the uncertainties of the VPP scheduling and the impacts of capacity withholding process. The main contributions of this paper can be summarized as follows:

- The proposed model uses a stochastic optimization framework for the optimal operational scheduling of a microgrid-based VPP.
- The uncertainties of the VPP operational variables considered are the thermal and electrical demands, the wholesale market prices, the plug-in hybrid electric vehicle (PHEV) charge and discharge values, and also the generation of photovoltaic (PV) arrays and wind turbines (WTs).
- The impact of the capacity withholding index on the scheduling problem is determined.

The rest of this manuscript is organized as follows: Section 2, the model of the problem is described and the details of the proposed approach are introduced. In Section 3 the simulation results are addressed and discussed. Finally, the conclusion is drawn in Section 4.

II. Problem Modeling and Formulation

The VPP comprises multi-MGs that sells active power, reactive power, and reserve to the upward electricity market. It is assumed that each microgrid is equipped with combined heat and power (CHP) units, fossil-fueled distributed generation (DG) facilities, WTs, PV arrays, electrical energy storage systems (ESSs), thermal storage systems (TSSs), boilers, and PHEV parking lots.

The uncertainties of the VPP operational variables are the thermal and electrical demands, wholesale market prices, PHEV charge and discharge values, and electricity generation of PVs and WTs [11]. The Distribution System Operator (DSO) utilizes demand response programs (DRPs) to change the electricity load curves and it purchases electricity from the upward electricity market. The DSO electricity generation facilities are PV arrays, WTs, and DGs.

A. Wind Turbine Model

The wind turbine can be modeled as follows [12]:

$$P_w = \begin{cases} 0 & if\ \ v^{Wind} \le v_c^{Wind} \text{ or } v^{Wind} \ge v_f^{Wind} \\ P_r^{Wind}\dfrac{(v^{Wind}-v_c^{Wind})}{(v_r^{Wind}-v_c^{Wind})} & if\ \ v_c^{Wind} \le v^{Wind} \le v_r^{Wind} \\ P_r^{Wind} & otherwise \end{cases} \quad (1)$$

where v^{Wind} is the wind speed, $v_c{}^{Wind}$ is the cut-in speed, $v_r{}^{Wind}$ is the rated speed, $v_f{}^{Wind}$ is cut-out speed, and $P_r{}^{Wind}$ is rated power of wind turbine.

B. Photovoltaic Array Model

The maximum power output of PV array can be written as [12]:

$$P^{PVA} = A^{PVA}\cdot\eta\cdot I(1-0.005(t_0-25)) \quad (2)$$

where A^{PVA} is the PV array area, η is the PV array energy conversion efficiency, I is the solar irradiation, and t_0 is the ambient temperature.

C. Combined Heat and Power Model

The nonlinear feasible operating region for CHP units can be presented as:

$$\alpha_{CHP}^{'}\cdot P^{CHP} + \beta_{CHP}^{'}\cdot Q^{CHP} \ge \gamma_{CHP}^{'} \quad (3)$$

where $\alpha_{CHP}^{'}, \beta_{CHP}^{'}, \gamma_{CHP}^{'}$ are the coefficient of heat-power feasible region for the CHP units. The detailed model of CHP units is available in [12].

D. Plug-in Hybrid Electric Vehicle Model

The PHEV charge and discharge is a stochastic process that its energy balance and constraints can be written as [12]:

$$\begin{aligned} EN_{PHEV}(t) = EN_{PHEV}(t-1) + \\ \varpi_{PHEV}^{Charge}\cdot PCH_{PHEV}(t)\cdot\Delta t \\ -\frac{1}{\varpi_{PHEV}^{Discharge}}\cdot PDCH_{PHEV}\cdot\Delta t \end{aligned} \quad (4)$$

$$EN_{PHEV}{}^{min} \le EN_{PHEV} \le EN_{PHEV}{}^{max} \quad (5)$$

$$\begin{aligned} 0 \le PCH_{PHEV} \le PCH_{PHEV}^{Max} \\ 0 \le PDCH_{PHEV} \le PDCH_{PHEV}^{Max} \end{aligned} \quad (6)$$

$$EN_{PHEV}(t) = \sigma\cdot EN_{PHEV}{}^{max} \qquad \forall\ t = t_{Departure} \quad (7)$$

where ϖ_{PHEV}^{Charge} and $\varpi_{PHEV}^{Discharge}$ are the charge and discharge limitation ratio, respectively. The PCH^{PHEV} and $PDCH^{PHEV}$ variables are the PHEV's power of charge and discharge, respectively. Eq. (4) presents the energy balance of PHEV battery. Eq. (5) and Eq. (6) present the limits of charge and discharge rates of PHEV battery and σ is the expected coefficient [12]. The EN_{PHEV} is the PHEV's energy storage content.

E. Demand Response Programs

It is assumed that the VPP can participate in DRPs that comprise time-of-use (TOU) and direct load control (DLC) procedures. The VPP loads consist of critical, deferrable, and controllable loads. Thus, the DRP process model can be presented as [12]:

$$P_{VPP}^{Load} = P_{VPP\ Critical}^{Load} + P_{VPP\ Deferrable}^{Load} + P_{VPP\ Controllable}^{Load} \quad (8)$$

$$\Delta P_{VPP}^{TOU} = P_{VPP\ Deferrable}^{Load} \quad (9)$$

$$\sum_{t=1}^{NPeriod} \Delta P_{VPP}^{TOU} = 0 \quad (10)$$

$$\Delta P_{VPP\ Min}^{TOU} \le \Delta P_{VPP}^{TOU} \le \Delta P_{VPP\ Max}^{TOU} \quad (11)$$

$$\Delta P_{VPP\ Min}^{DLC} \le \Delta P_{VPP}^{DLC} \le \Delta P_{VPP\ Max}^{DLC} \quad (12)$$

$$\Delta P_{VPP\ Max}^{DLC} = P_{VPP\ Controllable}^{Load} \quad (13)$$

$$P_{VPP}^{DRP} = \Delta P_{VPP}^{DLC} + \Delta P_{VPP}^{TOU} \quad (14)$$

Eq. (8) terms are the VPP critical load, deferrable load, and controllable electrical load, respectively. Eq. (9) denotes that the change of TOU power is equal to the deferrable load.

Eq. (10) presents that the sum of the TOU electrical load changes is equal to zero. Eq. (11) and Eq. (12) present the maximum and minimum limits of TOU and DLC variables, respectively. Further, Eq. (13) presents that the maximum value of the DLC control variable is equal to the VPP controllable electrical load. Finally, the VPP loads that can participate in the DRP process are presented as Eq. (14).

Authorized licensed use limited to: b-on: UNIVERSIDADE DO PORTO. Downloaded on July 30,2021 at 17:19:45 UTC from IEEE Xplore. Restrictions apply.

F. Capacity Withholding Detection Process

The VPP can withhold its capacity in the retail electricity market to increase the price of electricity when the price of the wholesale market is higher than the price of electricity in the retail market. The DSO should detect the capacity withholding process, prevent it through an ex-ante way, and penalize it. Thus, the VPP operator should consider the capacity withholding process of MGs in his/her optimal day-ahead scheduling to reduce the penalties. The aggregate demand function can be written as (15):

$$x = -\alpha Y + \beta, \qquad \alpha > 0 \tag{15}$$

where α and β are the parameters of the demand curve. The π and Y variables are the price and quantity of load, respectively. It is assumed that in the SFE (supply function equilibrium) game model each VPP submit its bid in the following form [13]-[15]:

$$y = \frac{1}{\sigma}(\pi - \eta), \qquad \sigma > 0 \tag{16}$$

where σ and η are the parameters of VPP submitted bid. The capacity withholding index (*CWI*) of Refs. [13, 14] is considered to detect the withholding process of the VPP that can be presented as (17):

$$CWI = \frac{\Delta Y^{distort}}{\Delta Y^{withheld}} = \left(\frac{1}{1+\sum_{i=1}^{N}\frac{\alpha}{a_i}}\right)\left(\frac{\sum_{i=1}^{N}\left(\frac{y_i^e}{a_i\hat{A}_i}+\frac{\Delta\lambda_i^{distort}}{a_i}\right)}{\sum_{i=1}^{N}\left(\frac{y_i^e}{a_i\hat{A}_i}+\frac{\Delta\lambda_i^{withheld}}{a_i}\right)}\right) \tag{17}$$

where $\Delta Y^{distort}$ and $\Delta Y^{withheld}$ are the capacity distortion of the market and capacity withheld of the market, respectively. $\Delta\lambda^{distort}$ and $\Delta\lambda^{withheld}$ are the Lagrangian multipliers associated with power balance constraints in the distortion of market and capacity withheld of market conditions, respectively.

N and *a* are the number of microgrids and their generation cost multiplier, respectively. The e index stands for the Oligopoly market equilibrium point. Further, $\hat{A}$ can be presented as (18):

$$\hat{A}_i = \frac{1}{\sigma} + \sum_{j=1,\ i\neq j}^{N}\frac{1}{\sigma_j} \tag{18}$$

G. The First Stage Optimization Objective Function

The first stage objective function maximizes the VPP profit for the day-ahead energy and ancillary service markets that can be written as (19):

$$Max\ profit_{VPP} = \sum_{NOS} prob(REV_{VPP} - C_{VPP}) \tag{19}$$

where, NOS is the number of operational state scenarios. Eq. (19) terms can be written as (20):

$$\begin{aligned} REV_{VPP} = {} & \omega_{VPP}^{DA}\cdot Cap_{VPP}^{DA} + \chi_{VPP}^{DA}\cdot P_{VPP}^{DA} \\ & + \chi'^{DA}_{VPP}\cdot Q_{VPP}^{DA} + \varpi_{VPP}^{DRP}\cdot Cap_{VPP}^{DRP} \\ & + \zeta_{VPP}^{DRP}\cdot P_{VPP}^{DRP} + \zeta'^{DRP}_{VPP}\cdot Q_{VPP}^{DRP} \end{aligned} \tag{20}$$

$$\begin{aligned} C_{VPP} = {} & C_{MGs}^{CHPs} + C_{MGs}^{PVAs} + C_{MGs}^{WTs} + C_{MGs}^{ESSs} + C_{MGs}^{TSSs} + \\ & C_{MGs}^{PHEVs} + C_{MGs}^{DGs} + C_{MGs}^{Boilers} + Penalty \end{aligned} \tag{21}$$

In (20), the $\omega_{VPP}^{DA}, \chi_{VPP}^{DA}, \chi'^{DA}_{VPP}$ parameters are the reserve price, active power price, and reactive power price, respectively. The $Cap_{VPP}^{DA}, P_{VPP}^{DA}, Q_{VPP}^{DA}$ variables are the accepted values of VPP's reserve, active power, and reactive power volumes by the DSO.

The $\varpi_{VPP}^{DRP}, \zeta_{VPP}^{DRP}, \zeta'^{DRP}_{VPP}$ parameters are the capacity fee of DRP contribution, active power fee of DRP, and reactive power fee of DRP, respectively. The $Cap_{VPP}^{DRP}, P_{VPP}^{DRP}, Q_{VPP}^{DRP}$ variables are the values of DRP capacity, active power, and reactive power volumes.

The $C_{MGs}^{CHPs}, C_{MGs}^{PVAs}, C_{MGs}^{WTs}, C_{MGs}^{ESSs}, C_{MGs}^{TSSs}, C_{MGs}^{PHEVs}, C_{MGs}^{DGs}, C_{MGs}^{Boilers}$ variables are the costs of MGs' CHPs, PV arrays, WTs, ESSs, TSSs, PHEVs, boilers, and DGs, respectively. The *prob* parameter is the probability of the scenario. The *penalty* parameter is determined by the DSO for capacity withholding.

H. The Second Stage Optimization Objective Function

The second stage objective function minimizes the DSO energy procurement costs for the day-ahead energy and ancillary service markets considering capacity withholding of VPPs that can be written as (22):

$$Min\ \mathbf{Z}_{DSO} = \sum_{NOS} prob\cdot[W_1\cdot C_{DSO} + W_2\cdot CWI] \tag{22}$$

From Eq. (22), the terms can be written as (23):

$$\begin{aligned} C_{DSO} = {} & \omega_{VPP}^{DA}\cdot Cap_{VPP}^{DA} + \sum\chi_{VPP}^{DA}\cdot P_{VPP}^{DA} \\ & + \sum\chi'^{DA}_{VPP}\cdot Q_{VPP}^{DA} + \varpi_{VPP}^{DRP}\cdot Cap_{VPP}^{DRP} \\ & + \sum\zeta_{VPP}^{DRP}\cdot P_{VPP}^{DRP} + \sum\zeta'^{DRP}_{VPP}\cdot Q_{VPP}^{DRP} \\ & + \sum\zeta_{WM}^{DA}\cdot P_{WM}^{DA} + \sum\zeta'^{DA}_{WM}\cdot Q_{WM}^{DA} \\ & + C_{DSO}^{PVAs} + C_{DSO}^{WTs} + C_{DSO}^{DGs} \ - penalty \end{aligned} \tag{23}$$

In (23), the $\zeta_{WM}^{DA}, \zeta'^{DA}_{WM}$ parameters are the active power market price and reactive power market price, respectively. The P_{WM}^{DA}, Q_{WM}^{DA} variables are the purchased active power and reactive power volumes from the wholesale market by the DSO. The $C_{DSO}^{PVAs}, C_{DSO}^{WTs}, C_{DSO}^{DGs}$ variables are the costs of DSO PV arrays, WTs, and DGs, respectively. W_1 and W_2 are weighting factors. The DSO determines the thresholds of *CWI* and the VPP should not violate the determined *CWI* limits.

I. Constraints

The optimization algorithm considers the following constraints for the first and second stage problems:

- The electrical and thermal power balance for each scenario for the second stage problem:

$$P_{WM}^{DA} + P_{DSO}^{WTs} + P_{VPP}^{DA} \pm P_{VPP}^{DRP} + P_{DSO}^{PVAs} + P_{DSO}^{DGs} = P_{DSO}^{D} \tag{24}$$

$$Q_{WM}^{DA} + Q_{DSO}^{WTs} + Q_{VPP}^{DA} \pm Q_{VPP}^{DRP} + Q_{DSO}^{PVAs} + Q_{DSO}^{DGs} = Q_{DSO}^{D} \tag{25}$$

where in (24) and (25), P_{DSO}^{D}, Q_{DSO}^{D} are active and reactive demands of the distribution system.

- AC power flow equations are considered that are not presented for the sack of space [12].
- Limit of power generations for electricity generation facilities for the first and second stage problems:

$$P_{Min} \le P \le P_{Max} \tag{26}$$

where P_{Min} and P_{Max} are the minimum/maximum active power of the electricity generation facility, respectively.

- Limit of the thermal power of boilers:

$$Q'^{Boiler\ Min}_{Thermal} \le Q'^{Boiler}_{Thermal} \le Q'^{Boiler\ Max}_{Thermal} \tag{27}$$

where $Q'^{Boiler\ Min}_{Thermal}$ and $Q'^{Boiler\ Max}_{Thermal}$ are the minimum/maximum output of the boiler, respectively.

- The ESS and TSS limit and maximum charge and discharge rate constraints can be presented in (28) and (29), respectively.

Authorized licensed use limited to: b-on: UNIVERSIDADE DO PORTO. Downloaded on July 30,2021 at 17:19:45 UTC from IEEE Xplore. Restrictions apply.

These constraints are considered in the first stage problem. The Q' variable is the thermal energy of TSS.

$$P^{ESS} \le Capacity^{ESS} \quad (28)$$

$$Q'^{TSS}_{Thermal} \le Capacity^{TSS} \quad (29)$$

where $Capacity^{ESS}$ and $Capacity^{TSS}$ are the ESS and TSS facilities capacity, respectively. Eq. (30) and Eq. (31) present the charge and discharge ramp-rate limits of ESS, respectively.

The X and Y variables are the ESS binary variables that present the discharge and charge status of ESS, respectively. The X' and Y' variables are the TSS binary variables that present the discharge and charge status of TSS, respectively. Eq. (32) and Eq. (33) denote the charge and discharge ramp-rate limits of TSS, respectively.

$$P^{CH,ESS} \le P^{ESS}_{RATE\ CH} \cdot X \qquad X \in \{0,1\} \quad (30)$$

$$P^{DISCH,ESS} \le P^{ESS}_{RATE\ DISCH} \cdot Y \qquad Y \in \{0,1\} \quad (31)$$

$$Q'^{CH,TSS}_{Thermal} \le Q'^{TSS}_{RATE\ CH} \cdot X' \qquad X' \in \{0,1\} \quad (32)$$

$$Q'^{DISCH,TSS}_{Thermal} \le Q'^{TSS}_{RATE\ DISCH} \cdot Y' \qquad Y' \in \{0,1\} \quad (33)$$

where $P^{ESS}_{RATE\ CH}$ and $P^{ESS}_{RATE\ DISCH}$ are the charge/discharge rate of the ESS unit, respectively. $Q'^{TSS}_{RATE\ CH}$ and $Q'^{TSS}_{RATE\ DISCH}$ are the charge/discharge rate of the TSS unit, respectively.

The ESS and TSS charge/discharge constraints are presented as (34) and (35), respectively:

$$X + Y \le 1 \quad (34)$$

$$X' + Y' \le 1 \quad (35)$$

- Limits of power exchange with the upstream network:

$$P^{DA}_{WM} \le P^{EXCH}_{\max} \quad (36)$$

where P^{EXCH}_{max} is the maximum active power that could be exchanged with the upstream network.

- DRP operation constraints:

$$\Delta P^{DRP\ Min}_{VPP} \le \Delta P^{DRP}_{VPP} \le \Delta P^{DRP\ Max}_{VPP} \quad (37)$$

where $\Delta P^{DRP\ Min}_{VPP}$ and $\Delta P^{DRP\ Max}_{VPP}$ are the minimum/maximum load change in DRP, respectively. Fig. 1 depicts the procedure of the proposed optimization algorithm. The algorithm codes were developed in GAMS and MATLAB.

III. Simulation and Results

The 123-bus IEEE test system is considered to assess the model [12]. The system comprises six MGs, seven DGs, six CHPs, three PVAs, three WTs, five DRPs, and four PHEV parking lots. Fig. 2 presents the topology of the 123-bus IEEE test system. The technical and cost information of CHP units, TSSs, ESSs, and PV units are presented in [12].

MUs stands for Monetary Units. The boilers and TSS characteristics are available in [12]. The MGs may form multiple VPPs for different DA scheduling horizons to increase their market share and increase the electricity price.

Fig. 3 presents the aggregated electrical and heating loads of the 123-bus test system. Fig. 4 depicts the estimated values of active power price, reactive power price, and the reserve price for the day-ahead horizon. Table I presents the input parameters of the optimization process.

The VPP aggregates the bidding of its downward MGs and submits his/her bids to the DSO. Fig. 5 and Fig. 6 present the values of the MG_1-MG_3 bids and the accepted values of the MG_1-MG_3 for active power and reactive power, respectively. The maximum value of MG_1-MG_3 active power bids is 2320 kW that belongs to MG_2 for hour 17:00. Further, the maximum value of MG_1-MG_3 active power accepted bids is 1254 kW that belongs to MG_2 for hour 17:00.

Fig. 7 and Fig. 8 present the values of the MG_4-MG_6 bids and the accepted values of the MG_4-MG_6 for active power and reactive power, respectively. The maximum value of MG_4-MG_6 active power bids is 8553 kW that belongs to MG_6 for hour 17:00. Further, the maximum value of MG_4-MG_6 active power accepted bids is 4820 kW that belongs to MG_6 for hour 17:00. Fig. 9 depicts the 123-bus test system photovoltaic arrays and wind turbines electricity generation for the day-ahead horizon. The estimated energy generation of photovoltaic arrays and wind turbines are 8.229 MW and 14.962 MW, respectively.

Fig. 10 presents the accepted values of active power VPP bids, the 123-bus system active loads, the active power generation of DERs of DSO, and the DSO active power import from the wholesale market. The estimated values of the accepted active power bid of VPP and DERs active power generation are 89.368 MWh and 212.854 MWh, respectively.

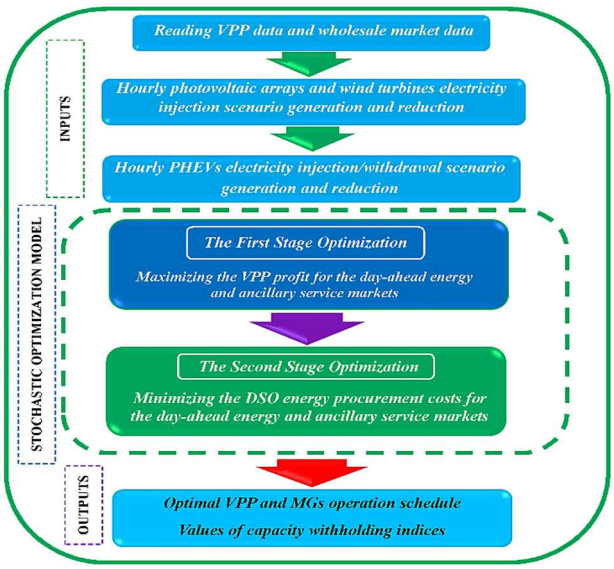

Fig. 1. Procedure of the proposed optimization algorithm.

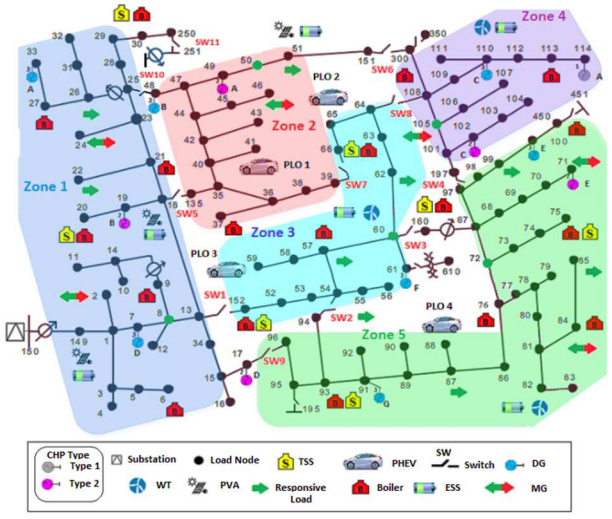

Fig. 2. The 123-Bus IEEE test system.

Authorized licensed use limited to: b-on: UNIVERSIDADE DO PORTO. Downloaded on July 30,2021 at 17:19:45 UTC from IEEE Xplore. Restrictions apply.

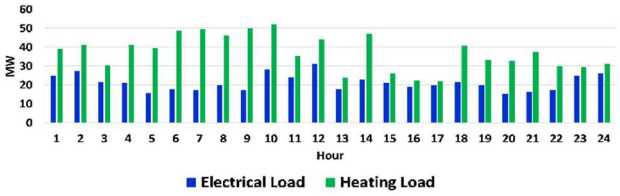

Fig. 3. The 123-bus IEEE test system electrical and heating loads.

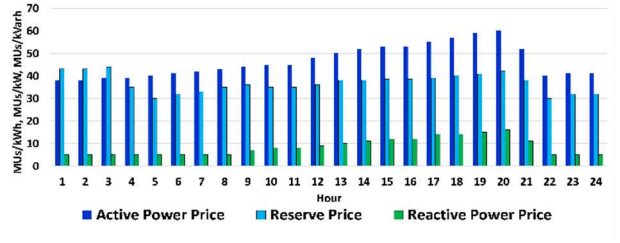

Fig. 4. Estimated values of wholesale energy and ancillary service prices.

TABLE I. THE OPTIMIZATION INPUT.

System parameter	Value
Number of solar irradiation scenarios	400
Number of wind turbine power generation scenarios	600
Number of PHEVs contribution scenarios	1500
Number of solar irradiation reduced scenarios	40
Number of wind turbine power generation reduced scenarios	60
Number of PHEVs contribution reduced scenarios	50

Fig. 5. The MG_1-MG_3 active power bids and the accepted values of bids.

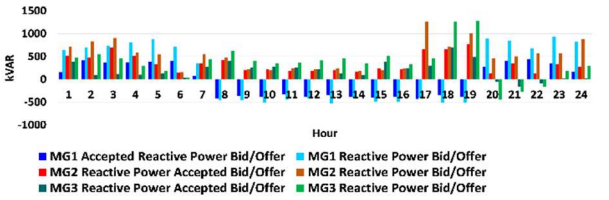

Fig. 6. The MG_1-MG_3 reactive power bids and the accepted values of bids.

Fig. 7. The MG_4-MG_6 active power bids and the accepted values of bids.

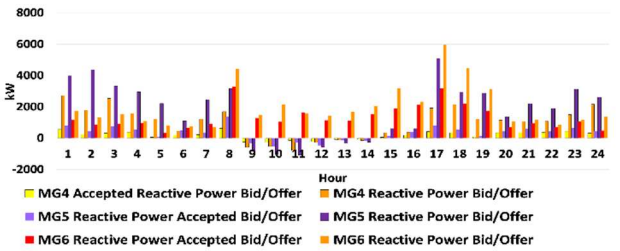

Fig. 8. The MG_4-MG_6 reactive power bids and the accepted values of bids.

Fig. 11 presents the accepted values of reactive power VPP bids, the 123-bus system reactive loads, the reactive power generation of DERs of DSO, and the DSO reactive power import from the wholesale market. The estimated values of the accepted reactive power bid of VPP and DERs reactive power generation are 54.184 MVARh and 133.236 MVARh, respectively.

Fig. 12 and Fig. 13 show the estimated values of TSSs and PHEV parking lots of charge and discharge, respectively. The net transacted energy of PHEV parking lots is 380.91 MWh. Fig. 14 and Fig. 15 present the active power and reactive power values of DRP groups for the planning horizon, respectively.

The net transacted active energy of DRPs is 3.3168 MWh. The net transacted reactive energy of DRPs is 1.606 MVARh. Fig. 16 depicts the VPP accepted values of reserve bids for the day-ahead scheduling horizon. Two cases are considered in the case study:

- Case 1: Optimization of VPP scheduling considering $W_2 = 0$.
- Case 2: Optimization of VPP scheduling considering $W_2 = 1$.

Fig. 17 presents the CWI values for the scheduling horizon with and without the proposed algorithm. The maximum values of CWI for scheduling horizon with and without the proposed algorithm are 0.1728 and 0.43, respectively. The proposed algorithm successfully reduced the CWI by about 59.81%. Table II presents the VPP profits/costs for two cases. By assessing Table II it is obvious that the penalties of VPP are reduced from case 1 to 2 due to considering CWI. The net profit of VPP is increased by about 26%.

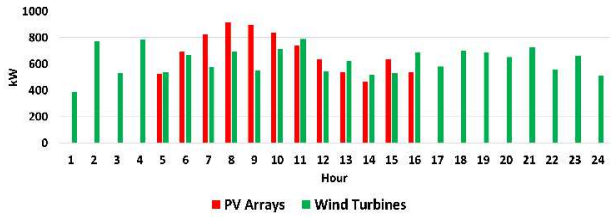

Fig. 9. The 123-bus test system photovoltaic arrays and wind turbines electricity generation for the day-ahead horizon.

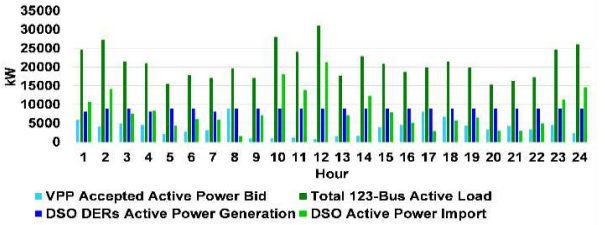

Fig. 10. The accepted values of active power VPP bids, the 123-bus system active loads, the active power generation of DERs of DSO, and the DSO active power import from the wholesale market.

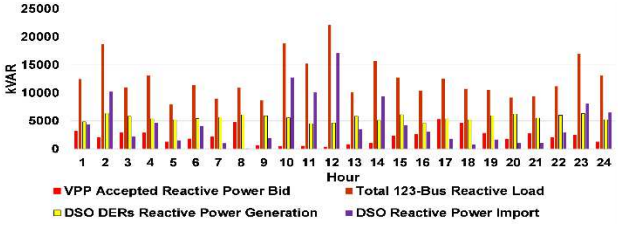

Fig. 11. The accepted values of reactive power VPP bids, the 123-bus system reactive loads, the reactive power generation of DERs of DSO, and the DSO reactive power import from the wholesale market.

Authorized licensed use limited to: b-on: UNIVERSIDADE DO PORTO. Downloaded on July 30,2021 at 17:19:45 UTC from IEEE Xplore. Restrictions apply.

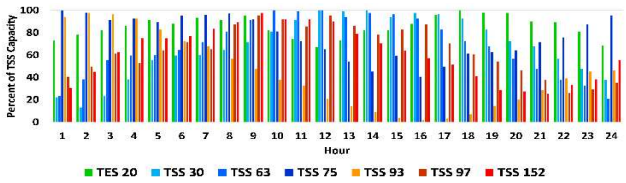

Fig. 12. The estimated values of TSSs charge and discharge.

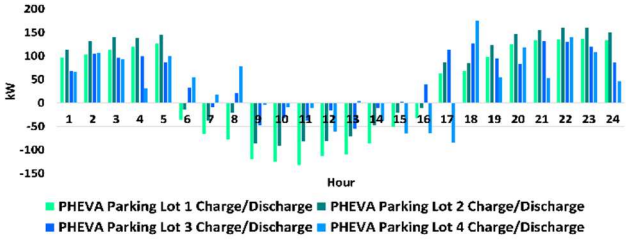

Fig. 13. The estimated values of PHEV parking lots charge and discharge.

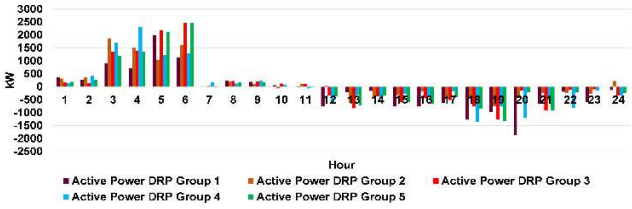

Fig. 14. The active power values of DRP groups for the planning horizon.

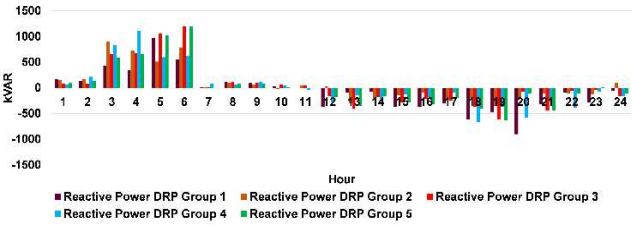

Fig. 15. The active power values of DRP groups for the planning horizon.

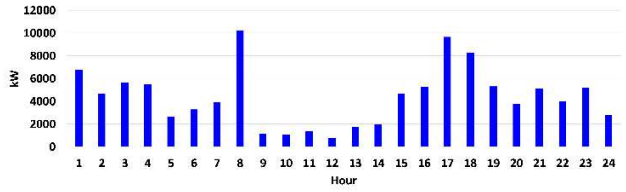

Fig. 16. The VPP accepted values of reserve bids for day-ahead scheduling horizon.

Fig. 17. The *CWI* values for scheduling horizon with and without the proposed algorithm.

TABLE III. THE VPP PROFIT FOR DIFFERENT CASES.

	Case 2 profits (MUs)	Case 1 profits (MUs)
Active Power	173710.1	199071.8
Reactive Power	18987	21683.16
Reserve	160505.2	185158.8
Penalties	-61033.4	-174165
Sum	292169	231749

IV. CONCLUSION

This work proposed a two-stage model for the optimal scheduling of microgrid-based virtual power plants, which transacted energy and ancillary services with the distribution system. The proposed model considered different energy sources such as photovoltaic arrays, wind turbines, and PHEVs. The capacity withholding opportunities of VPP was considered and a stochastic optimization process was utilized. The net profit of VPP was increased by about 26%. The authors are working on the real time ancillary service models to consider in the proposed optimization framework.

REFERENCES

[1] M. Vahedipour-Dahraie, H. Rashidizadeh-Kermani, A. Anvari-Moghaddam, P. Siano, "Risk-averse probabilistic framework for scheduling of virtual power plants considering demand response and uncertainties," *Elect. Power System Res.*, vol. 121: 106126, 2020.

[2] W. Guo, P. Liu, X. Shu, "Optimal dispatching of electric-thermal interconnected virtual power plant considering market trading mechanism", J. Cleaner Prod., vol. 279, 123446, 2021.

[3] B. Zhou, X. Liu, Y. Cao, C. Li, C.Y. Chung, K.W. Chan, "Optimal scheduling of virtual power plant with battery degradation cost," *IET Gen. Trans. Dist.*, vol. 10, pp. 712-725, 2016.

[4] J. Naughton, H. Wang, S. Riaz, M. Cantoni, P. Mancarella, "Optimization of multi-energy virtual power plants for providing multiple market and local network services," *Elec. Power Syst. Res.*, vol. 189, 106775, 2020.

[5] L. Ju, H. Li, J. Zhao, K. Chen, Q. Tan, Z. Tan, "Multi-objective stochastic scheduling optimization model for connecting a virtual power plant to wind-photovoltaic-electric vehicles considering uncertainties and demand response," *Energy Conv. Manag.*, vol. 128, pp.160-177, 2016.

[6] C. Wei, J. Xu, J. Liao, Y. Sun, Y. Jiang, D. Ke, Z. Zhang, J. Wang, "A bi-level scheduling model for virtual power plants with aggregated thermostatically controlled loads and renewable energy," *Appl. Energy*, vol. 224, pp. 659-670, 2018.

[7] S. Hadayeghparast, A. SoltaniNejad Farsangi, H. Shayanfar, "Day-ahead stochastic multi-objective economic/emission operational scheduling of a large-scale virtual power plant," *Energy*, vol. 172, pp. 630-646, 2019.

[8] X. Kong, J. Xiao, C. Wang, K. Cui, Q. Jin, D. Kong, "Bi-level multi-time scale scheduling method based on bidding for multioperator virtual power plant," *App. Energy*, vol. 24, pp. 178-189, 2019.

[9] A. Alahyari, M. Ehsan, M. Mousavizadeh, "A hybrid storage-wind virtual power plant (VPP) participation in the electricity markets: A self-scheduling optimization considering price, renewable generation, and electric vehicles uncertainties," *J. Energy Storage*, vol. 25, 100812, 2019.

[10] M. Foroughi, A. Pasban, M. Moeini-Aghtaie, A. Fayaz-Heidari, "A bi-level model for optimal bidding of a multi-carrier technical virtual power plant in energy markets," *Elec. Power Syst. Res.*, vol. 125, 106397, 2020.

[11] J. Ju, J. Tan, J. Yuan, Q. Tan, H. Li, F. Dong, "A bi-level stochastic scheduling optimization model for a virtual power plant connected to a wind–photovoltaic–energy storage system considering the uncertainty and demand response," *App. Energy*, vol. 171, pp. 184-199, 2016.

[12] A. Bostan, M. Setayesh Nazar, M. Shafie-khah, J.P.S. Catalão, "An integrated optimization framework for combined heat and power units, distributed generation and plug-in electric vehicles," *Energy*, vol. 202, 117789, 2020.

[13] S. Salarkheili, M. Setayesh Nazar, "New indices of capacity withholding in power markets", *Int. Trans. Electr. Energy Syst.*, vol. 25, 180-196, 2015.

[14] S. Salarkheili, M. Setayesh Nazar, "Capacity withholding analysis in transmission constrained electricity markets", *IET Gen. Trans. Dist.*, vol. 10, pp. 487-495, 2016.

[15] S. Qaeini, M.S. Nazar, M. Shafie-khah, G.J. Osório, J.P.S. Catalão, "Optimal planning of CHP-based microgrids considering DERs and demand response programs", *2020 IEEE 20th Mediterranean Electrotechnical Conference (MELECON)*, 2020.

Authorized licensed use limited to: b-on: UNIVERSIDADE DO PORTO. Downloaded on July 30,2021 at 17:19:45 UTC from IEEE Xplore. Restrictions apply.